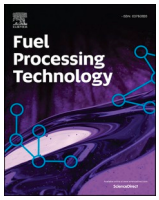
Fuel Processing Technology 291 (2026) 108547



Contents lists available at ScienceDirect

Fuel Processing Technology

journal homepage: www.elsevier.com/locate/fuproc



Implementing oxyfuel combustion in waste-to-energy: Analysis of flue gas recirculation strategies using a combined modeling and thermal analysis approach

Isabel Kaphahn *, Peter Quicker

Thermoprocesses and Emission Control in Waste Management and Recycling, Teaching and Research Unit, RWTH Aachen University, 52062 Aachen, Germany

ARTICLE INFO

Keywords:
Oxyfuel combustion
Flue gas recirculation
MSW
WtE
Thermogravimetric analysis
$O_2/CO_2/H_2O$ atmosphere

ABSTRACT

Given the potential of oxyfuel combustion for carbon capture, the impact of flue gas recirculation on oxyfuel combustion in Waste-to-Energy is investigated using a combined modeling and thermoanalytical approach, providing the basis for technical implementation. The oxyfuel combustion model reveals distinct gas compositions and flow rates for different recirculation strategies. Recirculation before flue gas treatment results in high pollutant concentrations in the oxidizer mixture but reduces the volume flow in downstream units. Recirculation after flue gas treatment lowers pollutant levels and, as in the first case, shows high H_2O concentrations in the oxidizer mixture. Dry flue gas recirculation achieves the highest CO_2 concentration but also the highest relative N_2 content in the clean, dry flue gas. By recirculating a larger absolute amount of O_2 to the oxidizer mixture, dry recirculation reduces the O_2 demand by 11.6% compared with wet recirculation. Thermogravimetric and differential thermal analysis of refuse-derived-fuel examines the influence of O_2 and H_2O concentrations on combustion performance. Increasing O_2 concentration strongly promotes char combustion, while devolatilization is slightly affected. Achieving similar combustion and burnout as with air, requires 32–35 vol-% O_2 in CO_2. Higher H_2O content slightly enhances char combustion, indicating a positive effect of the wet recirculation.

1. Introduction

As part of the European Green Deal, the European Union has committed to achieving climate neutrality by 2050 with an intermediate target of reducing greenhouse gas emissions by at least 55% until 2030, including the Waste-to-energy (WtE) sector [1]. WtE plants contribute to climate and resource protection by supplying energy, recovering metals, and reusing residues in construction [2,3]. In 2023, 511 kg of municipal solid waste (MSW) per capita have been generated in the EU, of which 129 kg per capita were incinerated [4]. CEWEP counts 100 million tons of thermally treated waste in 498 WtE plants (excluding hazardous waste incineration) in Europe [5]. In Germany, an above-average amount of 601 kg waste per capita has been generated [4], of which 26.2 million tons of waste were thermally treated in 68 WtE plants and 36 SRF-powerplants in 2021 [2,6]. The emission of CO_2 during waste incineration is estimated to be about 0.84 tons of CO_2 per ton of waste incinerated [6]. Due to different waste compositions and resulting carbon content, another study refers to 1.1 tons of CO_2 per ton of waste incinerated [7]. The emitted CO_2 is differentiated by fossil or biogenic origin. Approximately 50–60% of CO_2 emissions are estimated to be of biogenic origin, while the remaining CO_2-emissions are of fossil origin [8].

To achieve climate neutrality carbon capture technologies are being evaluated for WtE plants. Three different carbon capture routes could theoretically be applied: pre-combustion, post-combustion and oxyfuel. While post-combustion and oxyfuel could theoretically be retrofitted, pre-combustion defines the gasification of waste to obtain syngas [9]. Post combustion carbon capture is integrated to capture CO_2 from the flue gas, without the need for modifications in the upstream process. It is widely accepted that amine based absorption processes are currently the most mature technology, with the first industrial application in Duiven (Netherlands) and numerous feasibility and pilot plant studies as listed by Poretti and Stengler [3,10]. A range of other post combustion technologies currently possessing lower technology readiness levels, is currently under investigation, e.g. the hot-potassium-carbonate process or enzyme-based capture [3,11]. Oxyfuel technology for carbon capture involves the utilization of pure oxygen with recirculated flue gas as the oxidant instead of air. Thereby, the oxygen is diluted to maintain similar

* Corresponding author.
E-mail address: kaphahn@teer.rwth-aachen.de (I. Kaphahn).

https://doi.org/10.1016/j.fuproc.2026.108547
Received 5 January 2026; Received in revised form 9 July 2026; Accepted 23 July 2026
Available online 29 July 2026
0378-3820/© 2026 The Authors. Published by Elsevier B.V. This is an open access article under the CC BY-NC-ND license (http://creativecommons.org/licenses/by-nc-nd/4.0/).

combustion conditions compared to operation with air. The objective is to generate a flue gas with high CO_2 and H_2O content, which can be removed by condensation. Subsequent purification processes are employed to eliminate residual impurities [9,10]. In general, a variety of fuels can be utilized for oxyfuel combustion. In the past, oxyfuel combustion of coal has been studied in detail and was tested in demonstration plants up to 30 MW_{th} in CFB (CIUDEN, Spain) or PC fired boiler (Schwarze Pumpe, Germany). An overview of the pilot and demonstration plants is listed in [12]. Retrofitting oxyfuel combustion needs further components such as an oxygen supply unit, flue gas recirculation (FGR) unit and CO_2 compression and purification unit (CPU) [13]. The O_2 is typically supplied by an air separation unit based on a cryogenic distillation process with high energy demand. As an alternative, the usage of O_2 produced as a byproduct in water electrolysis for hydrogen production is currently being investigated [14–20]. For FGR, many configurations are considered, which mainly differ by wet or dry recirculation. Further, the exact positioning of the extraction for the recirculated flue gas stream decides for low/high dust loading, temperature and pollutant concentration. For coal combustion, primary and secondary recirculation streams have been considered, with a total recirculation rate of 60–80% of the flue gas [13,21]. The obtained flue gas contains high amounts of CO_2 and H_2O, followed by excess O_2, inert gases N_2 and Ar from air leakages, and impurities such as NO_x, SO_x, trace metals and others [22,23]. To meet CO_2 purity requirements, e.g. for transport or synthesis, a CPU is used, typically involving drying and cleaning of the flue gas, followed by compression and distillation, with the exact configuration depending on the required purity [12,24,25].

Numerous studies on oxyfuel combustion of coal have investigated the influence of oxyfuel technology on the combustion process, leading to several review papers such as [12,13,21,26]. In general, the replacement of N_2 by CO_2 and H_2O affects combustion process and heat transfer because of different physical and chemical properties. Due to the higher molar heat capacity of CO_2 (56.8 J/molK at 1000 °C) vs. N_2 (34.0 J/molK at 1000 °C) and the chemical reactivity of CO_2, at similar oxygen concentrations, the adiabatic flame temperature in oxyfuel combustion is reduced compared with air combustion. It is widely acknowledged that in order to achieve comparable combustion performances to those attained in air, the O_2 concentration needs to be increased to approximately 30 vol.-%. However, slight differences can be observed depending on the type of fuel, e.g. for different types of coal, oxygen concentrations of 25–42 vol.-% were determined. [9,13,26–28].

Depending on the FGR strategy, with wet recirculation the water vapor content in the combustion atmosphere is increased to 10–40 vol.-%. [29]. Only few studies have investigated the influence of water vapor on the combustion process. Reduced specific molar heat capacity of H_2O (44.5 J/molK at 1000 °C) vs. CO_2 (56.8 J/molK at 1000 °C) and higher O_2 diffusivity in H_2O than in CO_2 could affect combustion parameters. Further, less CO_2 and more H_2O could shift the chemical equilibrium of the exothermic water-gas shift reaction toward CO_2 and H_2 production, while more H_2O could promote endothermic char-H_2O gasification reactions [27,30]. Experimental lab-scale studies with coal and biomass yielded divergent results regarding the impact of water vapor content on the ignition [27,31–34]. However, the combustion temperature was generally observed to be increased, most likely because of the lower molar heat capacity and higher O_2 diffusivity [27,35,36]. In conjunction, an overall increased reactivity in comparison with a dry combustion atmosphere was detected, but more pronounced at lower oxygen levels [33,37,38]. Dueso et al. observed similar reactivity in wet or dry conditions at 30 vol.-% O_2 [37]. The impact on the overall burnout time and rate was found to be divergent [27,30,32–34,36,39]. Although char-H_2O reactions rates are four times higher than char-CO_2 reactions, the impact of H_2O is a subject of discussion [35]. Char gasification could contribute to 20–30% of char consumption [40], but char-O_2 reactions are by far the most relevant [30]. Endothermic gasification reactions have the potential to reduce particle temperature and extend burnout time, while the gas phase products could oxidize more rapidly and promote combustion [30,31,40].

Few studies have investigated the oxyfuel combustion of waste. The transferability to waste as a fuel is difficult due to the heterogenous composition [41]. Additionally, the firing technology is significantly different as globally around 80% of WtE plants are using grate firing [42]. A review of Wienchol et al. reveals that oxyfuel combustion is a feasible technology for implementing carbon capture at WtE plants [10]. Nevertheless, there are still many research questions to be investigated [10]. To date, experimental research involving waste or refuse-derived fuel (RDF) has been primarily conducted on a laboratory scale using thermogravimetric analysis or tube furnaces [43–54]. In general, thermogravimetric analysis of solid waste fractions has confirmed that the O_2 concentration in CO_2 needs to be elevated to achieve similar combustion performances as with air [43,44,46]. More extensive research has been carried out by Becidan et al. [41] using vertical tube furnace to analyze oxyfuel combustion of model MSW and Moreno et al. [55] using 200 kW_{th} CFB and SRF. To the best of the author's knowledge, Mack et al. 2023 [56] have thus far reported the only experimental investigation of oxyfuel combustion employing grate firing technology. While substantial RDF feeding issues caused pronounced fluctuations in the oxyfuel combustion process, stable operation was achieved when wood chips were used [56].

The implementation of oxyfuel combustion on an industrial scale in WtE plants has been the subject of only a limited number of studies conducting simulative research as listed in Table 1. Although wet and dry FGR strategies were incorporated within the simulations, the impact of different FGR strategies in WtE plants on the overall process has the need for further investigation [57]. Copik et al. 2024 developed a mathematical model of oxyfuel combustion in a grate furnace [58]. This model demonstrated that an increase in the oxygen content of the combustion atmosphere resulted in reduced burnout time, and higher temperatures in the grate and gas phase. Temperature regulation can be achieved by adapting the FGR rates [58]. Fu et al. 2025 analyzed the impact of air leakages, determining that the N_2 content in the flue gas is 26 vol.-% with 5% air leakage and decreases to 3.2 vol.-% with 0% air leakage [57]. The residual N_2 is mainly introduced by impurities in the oxygen supply. Reducing the N_2 concentration in the flue gas from 26 to 3.2 vol.-% decreases the specific power consumption of the CPU by 77%. This outcome highlights the importance of minimizing N_2 content in the flue gas released to CPU [57]. The majority of studies were conducted via ASPEN PLUS to investigate the implementation of oxyfuel combustion in WtE plants with different configurations, such as oxygen concentrations in the combustion atmosphere and excess oxygen ratio. In previous simulation studies, the FGR has been implemented at different positions within the process. However, a systematic comparison of these FGR strategies and a comprehensive assessment of their effects on the resulting gas composition have not yet been conducted, even though, these changes directly influence combustion behavior and downstream processes. Moreover, a systematic link to experimental research that evaluates the effects on combustion parameters is missing.

The present study thus proposes an oxyfuel combustion model of a WtE plant. The initial objective is to assess the impact of different FGR strategies on gas composition and molar flow rate throughout the process. The model is then used to conduct a sensitivity analysis to evaluate critical parameters such as CO_2 and N_2 content in the CPU inlet stream. Since the sensitivity analysis highlights the strong influence of the O_2 concentration in the oxidizer mixture (OM) on the overall process, as well as the significant dependence of the H_2O concentration in the OM on the selected FGR strategy, it is necessary to experimentally assess the effects of varying O_2 and H_2O levels on combustion behavior. Therefore, in a second step, Thermogravimetric Analysis (TGA) and Differential Thermal Analysis (DTA) of RDF are conducted to investigate the influence of varying O_2 and H_2O concentrations in the OM on the combustion characteristics. The overall aim is to establish a viable configuration by combining modeling and experimental approaches to achieve combustion behavior comparable to conventional air combustion, thereby

Table 1
Current research landscape of integrating oxyfuel combustion in WtE plants with grate firing technology.

Type of research	Author	Waste Capacity	Wet/Dry Flue Gas Recirculation	O_2 in Oxidizer Mixture [vol.-%]	Excess O_2 Ratio	Main Scope of Research
Aspen Plus Simulation	(Ding et al. 2018) [59]	800 t/d [WtE Shenzhen, China]	Dry	n.n	1.05	Process simulation, flue gas composition
Pro/II Simulation	(Vilardi et al. 2022) [60]	8.28 t/h	Dry	21, 40, 60 80, 99,6	n.n.	Exergy analysis, temperature and O_2-concentration in furnace
Aspen Plus Simulation (for the oxyfuel part)	(Huang et al. 2024) [18]	1000 t/day [WtE Foshan, Shina]	Dry	n.n	n.n	Process simulation with coupled electrolysis
Aspen Plus Simulation	(Sun et al. 2024) [61]	600 t/day	Dry	n.n	0.95–1.25	Process simulation with coupled supercritical CO_2 cycle and methanol production
Aspen Plus Simulation	(Fu et al. 2025) [57]	100,000 t/a [Haraldrud, Norway]	Wet	21.6	4 vol.-% excess oxygen in furnace outlet	Air leakage ratio, oxygen purity, comparison with MEA-process
Aspen Plus Simulation	(Re et al. 2025) [19]	374,000 t/a [Jätevoimala, Finland]	Wet	20.2	n.n	Coupling with water electrolysis,
Aspen Plus Simulation	(Peng et al. 2025) [20]	25 t/h [Foshan, China]	Dry	n.n	5 vol.-% excess oxygen in furnace outlet	Coupling with water electrolysis and dimethyl ether production, exergy efficiency
Mathematical modelling	(Copik et al. 2024)[58]	18 t/h [Kristiansand, Norway]	Wet	25, 33, 37, 43	n.n	Effect of FGR, oxygen distribution, oxidizer temperature

enabling the retrofitting of oxyfuel operation in WtE plants.

2. Methodology

2.1. Oxyfuel combustion model

A numerical model is adapted from conventional air combustion calculation to oxyfuel combustion using different FGR strategies. This idealized model is based on 100 recirculation steps to achieve steady-state conditions and is regulated by set O_2-concentration and O_2 excess ratio in the OM. The O_2 excess ratio is defined as the ratio of supplied oxygen to the stoichiometric oxygen requirement:

$$\lambda = \frac{\dot{n}_{O_2}}{\dot{n}_{O_2,stoich}} \tag{1}$$

The oxyfuel combustion calculation considers the FGR and its mixing with supplied oxygen and false air as shown in Fig. 1. Using a simplified mass balance approach, the stoichiometric combustion calculation considers the elements C, H, S, Cl, N, O, inherent moisture, and non-combustible ash. Minor components typically found in MSW, such as fluor, heavy metals (e.g., Pb, Zn, Cd, Hg), and trace organic pollutants, are not considered. The feedstock used in this study is a conventional MSW [62]. The complete combustion reaction is given as:

$$C_pH_qS_rN_sO_tCl_u + \left(p + \frac{q-u}{4} + r + \frac{15\%^*s}{2} - \frac{t}{2}\right) O_2 \rightarrow pCO_2 + \frac{q-u}{2}H_2O + rSO_2 + \frac{85\%^*s}{2}N_2 + 15\%^*sNO + u\,HCl \tag{2}$$

A detailed description of the model is given in 6.1 with intermediate calculation formulas listed in Table A.1. As illustrated in Fig. 1, State A is designated to raw gas composition after combustion and before flue gas

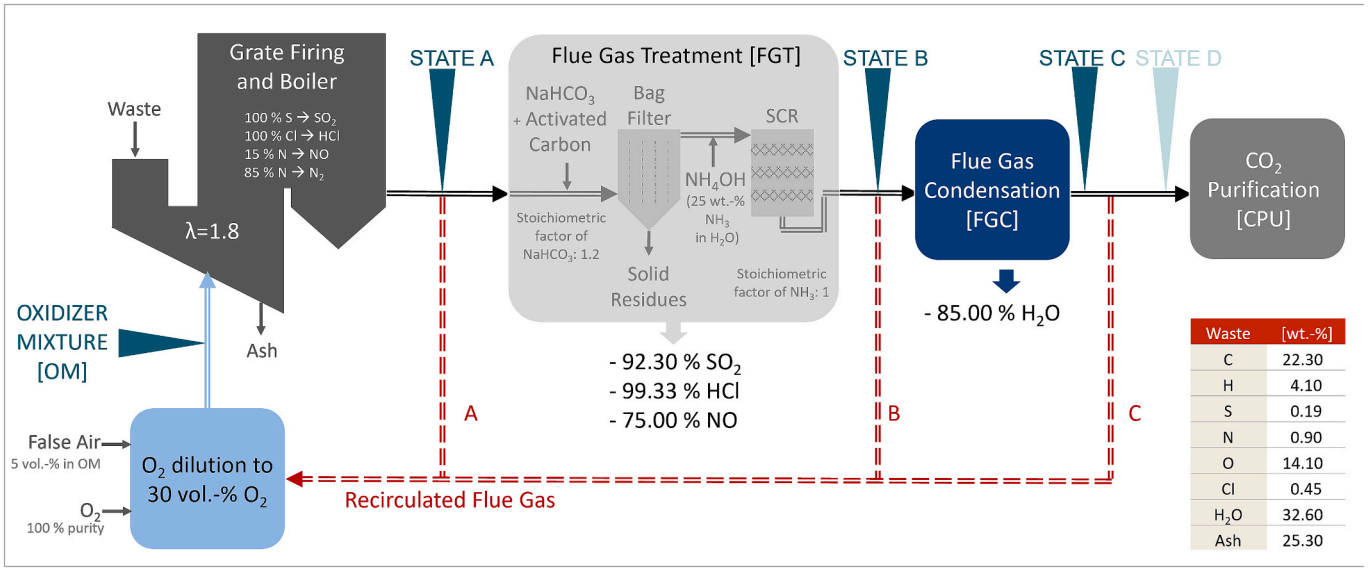


Fig. 1. Overview of oxyfuel combustion model and main assumptions.

treatment (FGT). FGT includes a dry sorption process with $NaHCO_3$ and activated carbon, and NO_x reduction by selective catalytic reduction (SCR) using injected NH_4OH. The FGT calculations were based on generally accepted reaction equations and efficiencies as presented in [63]. State B is designated to the cleaned flue gas after FGT before flue gas condensation (FGC). State C/D is designated to the dried and cleaned flue gas after FGC before CO_2 purification (CPU).

The different FGR strategies A, B and C as well as air combustion without recirculation are calculated and compared regarding gas composition and amount in the OM, and State A-D. Further, the impact of moisture, false air leakage, O_2 concentration (OM) and O_2 excess ratio on the dried clean gas composition sent to CO_2 purification (State D), the oxygen demand and the H_2O concentration in the OM is analyzed by conducting a sensitivity analysis of the base scenario.

2.2. Thermogravimetric and differential thermal analysis (TGA/DTA)

The combustion characteristics were studied using a LINSEIS STA PT1600/1000 to simultaneously record TGA and DTA. The furnace can heat the samples up to a temperature of 1600 °C, with a precision of 0.1 K. The thermocouple has a temperature resolution of 0.05 K and a temporal resolution of 0.1 s. The RDF was obtained from a German cement plant and grounded to a particle size of less than 1 mm. RDF was selected instead of untreated MSW because it provides a higher degree of reproducibility and homogeneity, which is essential for thermal analyses based on relatively small sample quantities. At the same time, RDF is still waste-derived and contains the same main combustible fractions as typical household waste, ensuring that the results remain representative for MSW combustion. The ultimate and proximate analyses are provided in Table 2. The initial sample weight was 10 mg ± 0.1 mg, contained in a 0.3 ml aluminum oxide crucible. The sample gas, which consisted of different mixtures of $CO_2/O_2/H_2O$ for oxyfuel experiments and $N_2/O_2/H_2O$ for reference air case, had a total constant flow rate of 50 ml/min. The purge gas N_2, which purges the weighing system and does not contact the sample, was kept at a constant flow rate of 75 ml/min. The sample was heated up from room temperature to 1000 °C with a constant heating rate of 10 K/min. The oxyfuel atmospheres analyzed were 21, 22.5, 25, 27.5, 30, 32.5 and 35 vol.-% O_2 in CO_2. At a constant O_2-concentration of 30 vol.-% the H_2O-concentration was varied from 0 to 10, 15, 20, 25, 30, 35 vol.-% in CO_2. As reference cases, 21 vol.-% O_2 in N_2 was analyzed with 0, 10, 20 and 30 vol.-% H_2O in CO_2. Each experiment was conducted in duplicate determination and the baseline of TGA and DTA was subtracted by average of four repetitions in Linseis TA Evaluation Software. The resulting TGA and DTA data curves were smoothed by Gaussian method (30 points). To obtain the Derivative Thermogravimetry (DTG), the discrete TGA data was derived by temperature and smoothed by Gaussian Method. The DTA electrical signal (μV) was calibrated by the calibration parameters to heat flow (mW). The calibration parameters were obtained by analyzing melting curves of Indium, Aluminum and Lead (Pb). The characteristic temperatures of DTG curves include DTG peak temperatures and the corresponding onset and offset temperatures, which were determined using the intersection method. The maximum weight loss rate of a peak is determined at peak temperature. To analyze the DTA curves, the peaks were individually analyzed using Linseis TA Evaluation software to determine onset, offset and peak temperatures (= characteristic temperatures). Because no enthalpies were determined, no further baseline correction was conducted. To analyze the characteristic temperatures as a function of O_2 concentration, linear trend lines were inserted using Microsoft Excel. The linear trend lines exceeding a coefficient of determination of $R^2 > 0.8$ were further evaluated to calculate the O_2/CO_2 atm required to achieve the characteristic temperatures of air. For this purpose, the average of the duplicate measurements of the characteristic temperature of air combustion served as the target y-value. The corresponding O_2 concentration (as x-value) was calculated with a 95% confidence interval.

Table 2
Ultimate and proximate analysis of the RDF used for TGA and DTA experiments.

Parameter	Unit	RDF	Methodology adapted from	Apparatus
Proximate analysis [raw (as-received) basis]				
Water	[wt.-%]	18.36	DIN EN 18134	drying oven
Ash	[wt.-%]	12.83	DIN 51719	muffle furnace (Nabertherm LH 30/14)
Volatiles	[wt.-%]	62.49	DIN EN 18123	muffle furnace (Nabertherm LH 30/14)
Lower Heating Value	[kJ/kg]	20.3	DIN EN ISO 18125	IKA C200
Ultimate analysis [dry, ash-free) basis]				
Carbon (C)	[wt.-%]	71.60	DIN 51732	Leco CHN-628
Hydrogen (H)	[wt.-%]	7.08	DIN 51732	Leco CHN-628
Nitrogen (N)	[wt.-%]	1.25	DIN 51732	Leco CHN-628
Sulfur (S)	[wt.-%]	0.97	DIN 51724	Leco SC 144 DR
Chlorine (Cl)	[wt.-%]	1.21	DIN 51727	Schott Titroline alpha

3. Results and discussion

3.1. Flue gas recirculation strategies

The modeling results demonstrate that the choice of FGR strategy has a substantial influence on both gas composition and volume flow rates throughout the oxyfuel combustion process. Fig. 2 illustrates pronounced differences in the gas composition and specific molar gas flow rates along the WtE process for the three evaluated FGR paths, with air combustion shown as a reference. The FGR strategies result in markedly different flue gas volume flows, as further quantified in Fig. 3. The corresponding FGR rates and the external oxygen demand are listed in Table 3.

Path A (recirculation after boiler, upstream of FGT) results in high pollutant concentrations in the OM. This configuration achieves the lowest flue gas volume in FGT and FGC, potentially reducing costs and energy demand for treatment because equipment sizing and fan power scale with volumetric gas flow, which directly determines absorber dimensions and gas-handling requirements [64]. On the contrary, the increased corrosive load in the OM may pose a risk to plant availability. This finding aligns with [56] who measured high HCl and SO_2 concentrations with wet recirculation before FGT, and concluded that pollutants should be removed before recirculation. Furthermore, Path A yields an OM with a high water vapor content (~ 40 vol.-%), which may impact combustion behavior and necessitates further investigation into its effects on combustion via TGA/DTA (see 3.2).

Path B (recirculation after FGT) exhibits a similar high H_2O content in the OM but with significantly reduced pollutant levels. The high water vapor content aligns with findings from Re et al. 2025 [19], who analyzed wet recirculation strategy. Although Path B requires treatment of a larger gas volume in the FGT, the reduced load in FGC represents a potential cost advantage in comparison with Path C due to smaller necessary condenser size and decreased auxiliary costs, as the required heat duty and corresponding heat exchanger area scale with the flue gas mass flow [65]. Both Path A and Path B result in a CO_2 concentration of 49.3 vol.-% in the clean, dry flue gas inlet to CPU [State D], accompanied by lower N_2 content (15.5 vol.-%) but higher O_2 (20.1 vol.-%) than Path C.

Path C (recirculation after FGC) differs fundamentally from A and B, with a very low H_2O content in the OM (3.5 vol.-%) and the highest CO_2

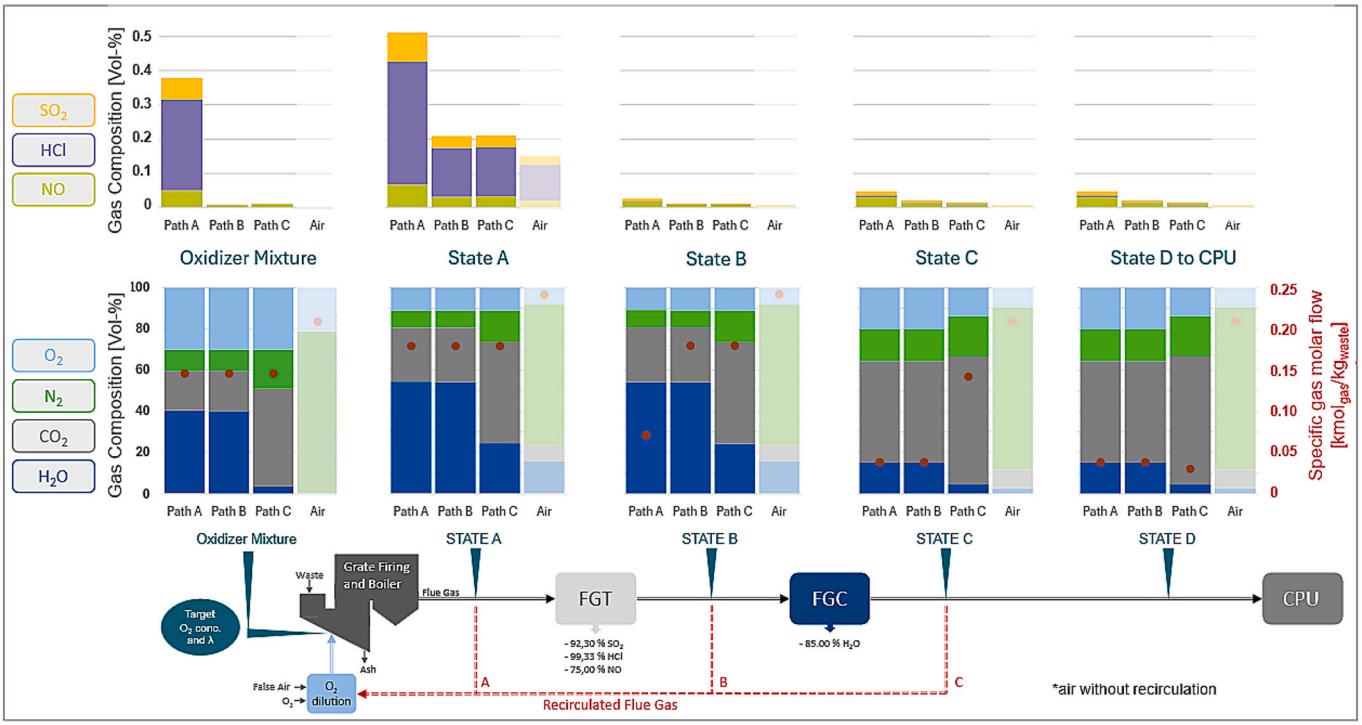


Fig. 2. Gas composition (columns) and specific molar flow (red dots) of oxyfuel combustion of different FGR strategies with base scenario and air as reference case. (For interpretation of the references to colour in this figure legend, the reader is referred to the web version of this article.)

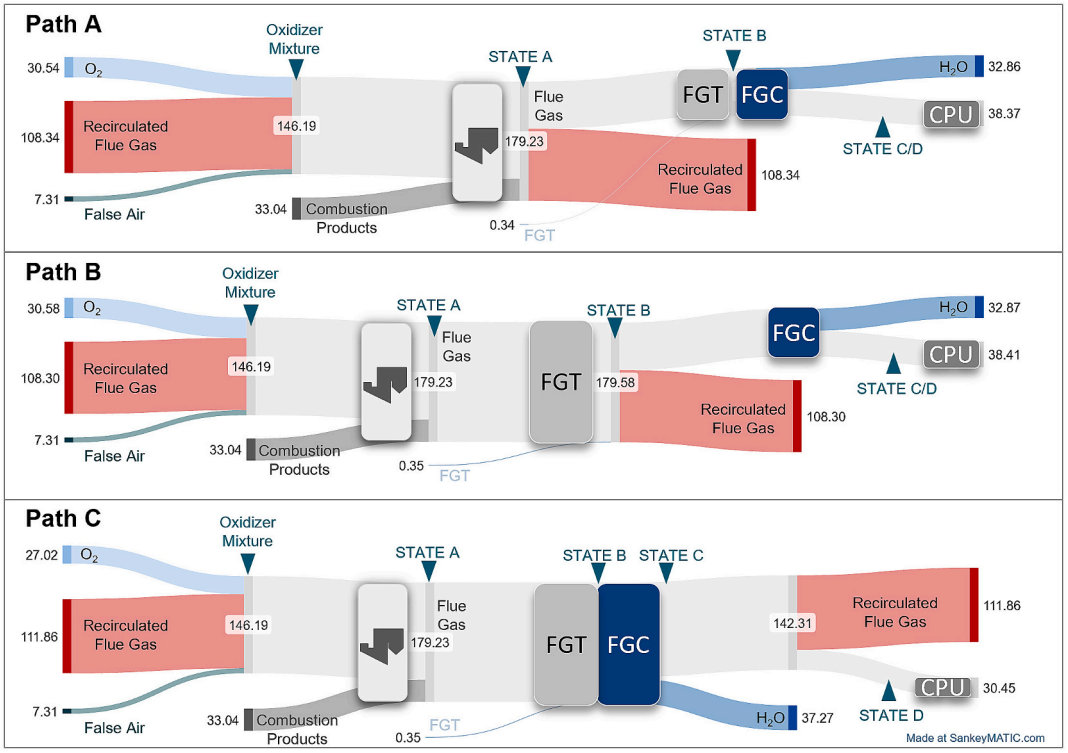


Fig. 3. Sankey diagram of relative gas volume flow in specific molar amount of gas [mol_{Gas}/kg_{Waste}] of different FGR strategies in oxyfuel combustion.

concentration in the CPU inlet stream (State D: 62.1 vol.-%). The higher CO_2 concentration in State D of Path C compared with Path A and B results from recirculation effects that reduce the total volume flow, while the molar amount of CO_2 of in State D remains constant across the different FGR strategies. This volume reduction occurs for two reasons. Firstly, less external oxygen is supplied because a larger absolute amount of O_2 is recirculated. Secondly, due to the differing volume flows and moisture contents, a greater amount of H_2O is condensed in Path C, further decreasing the volume flow in State D.

The sensitivity analysis as shown in Fig. 4 a) confirms that the excess

Table 3
FGR rate and amount of external oxygen demand of different FGR in oxyfuel combustion.

FGR Path	Unit	A	B	C
FGR rate	%	60.45	60.31	78.60
External O_2 demand	kgO_2/kgwaste	0.98	0.98	0.86

oxygen ratio is the dominant factor affecting **CO_2 concentration in the CPU inlet stream** [State D] with an exponential relationship because of recirculation effects. Reported CO_2 concentrations from simulation studies vary widely depending on oxygen ratio, recirculation strategy, and leakage assumptions. With dry FGR, Ding et al. [59] calculated 93.3 vol.-% CO_2 under very low excess oxygen ratio of 1.05, while with wet FGR, Fu et al. [57] reported 71.9 vol.-% CO_2 with 2.5 vol.-% leakage in their simulation study. Higher O_2 concentrations and increased excess oxygen ratios reduce N_2 content in State D via dilution, while air leakage significantly increases N_2 levels. This finding aligns with [66] who report air leakage is the primary source of N_2 in flue gas to CPU. The considered base scenario assumes a conservative leakage scenario. However, higher leakage rates are plausible, with empirical data from an exemplary German WtE plant showing air leakages of up to 16 vol.-% of the air inlet [67]. For wet recirculation, Fu et al. [57] calculated that N_2 content in the CPU inlet stream increases from 3.2 to 26 vol.-% when the air leakage increases from 0 to 5 vol.-%.

H_2O concentration in the OM is dominated by the choice of FGR

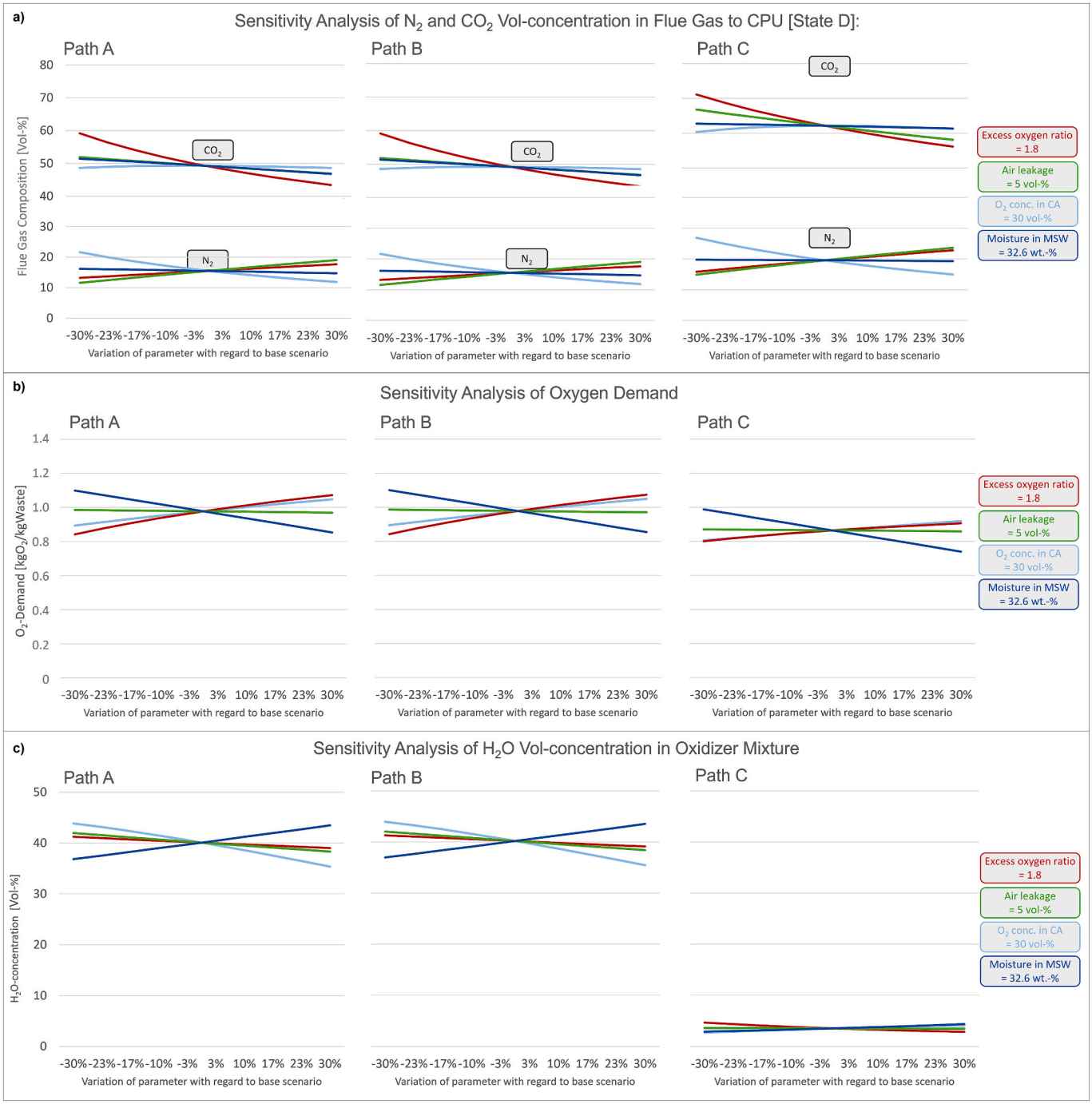


Fig. 4. Sensitivity analysis of a) CO_2 and N_2 content in the flue gas to CPU [State D], b) the oxygen demand and c) the H_2O concentration in the OM.

strategy, resulting in substantially higher H_2O content with wet FGR in Path A and B compared with dry FGR strategy Path C. Within the adopted FGR strategy, MSW moisture content and O_2 concentration are identified as the primary factors determining the H_2O content in the OM. This aligns with Copik et al. [58] who calculated lower H_2O content in the recirculated flue gas before mixing with O_2 (27.7 vol.-% compared to 54 vol.-% in Path A/B), attributable to the significantly lower MSW moisture (20 wt.-% vs. 32.6 wt.-% respectively).

Oxygen demand emerges as a further decisive factor for comparing FGR strategies. Path C requires ~11.6% less O_2 than Path A/B in the base scenario (0.86 kg_{O_2}/kg_{Waste} vs. 0.98 kg_{O_2}/kg_{Waste}, respectively), because a larger absolute amount of previously excess oxygen is recirculated to the OM. This is a result of the higher recirculation rate (A: 60.4 vol.-%, B: 60.3 vol.-%, C: 78.6 vol.-%) and the higher O_2 concentration in the recirculated flue gas (A: 10.9 vol.-%, B: 10.8 vol.-%, C: 13.7 vol.-%). The calculated recirculation rates are consistent with values reported in simulation studies [19,57,59] and practical coal combustion experiments, which indicate a range from 60 to 80 vol.-% [13]. O_2 demand scales strongly with the excess oxygen ratio but decreases with lower MSW moisture content. Air leakage has negligible influence on the oxygen demand, as it contributes additional O_2. These findings are consistent with [58] who observed increasing oxygen demand with higher O_2 concentrations in OM resulting in 0.64 kg_{O2}/kg_{Waste} (0.1 $kmol_{O2}/s$ with 18 t_{waste}/h). Compared with our study, the absolute oxygen demand calculated by Copik et al. [58] is significantly lower, which is attributable to a higher amount of ash (34.61 wt.-% vs. 25.30 wt.-%) and notably lower recirculation rates of 15–25% [58].

The present model is subject to several simplifications that may influence the interpretation of results. False air leakage is only accounted in the OM and not in downstream process sections, potentially

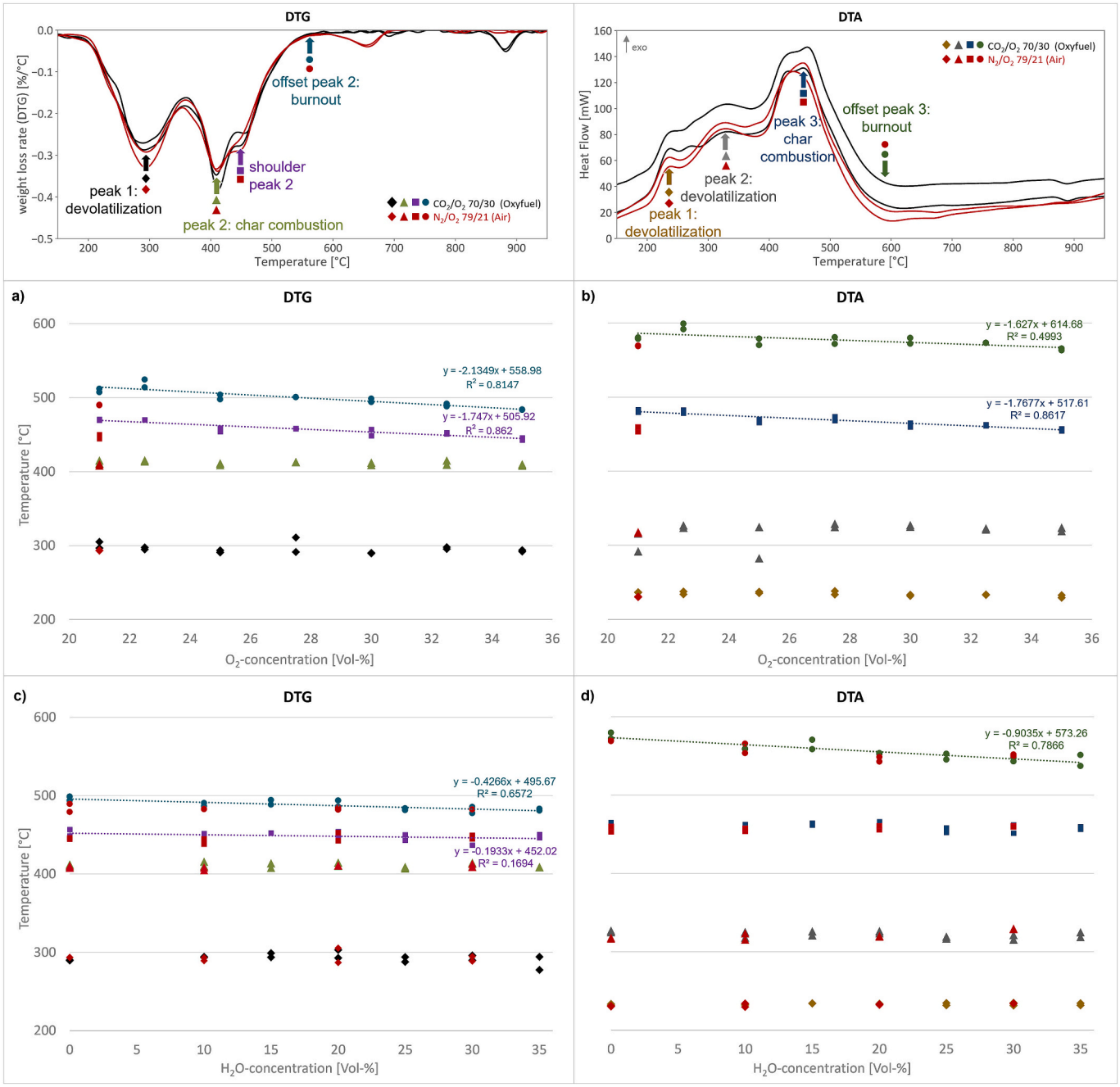


Fig. 5. Effect of O_2 and H_2O concentration on characteristic temperatures in DTG (a, c) and DTA (b, d).

underestimating its total impact. However, such contributions are expected to be reduced in oxyfuel systems through targeted technical measures and are therefore not explicitly considered in the present model, while air ingress by the waste feeding system remains unavoidable. The water condensation in FGC is represented by a fixed reduction percentage, without differentiation based on saturation vapor pressure. Further pollutant removal in the FGC is not considered. Potential NO_x reduction effects associated with FGR are not considered. Future studies will address the influence of alternative FGT designs and advanced FGR strategies such as recirculating between FGT components. The effect of varying pollutant concentrations and gas compositions on the effectiveness of the FGT system will be subject of detailed investigation. Further evaluation of energy demand will provide a more accurate assessment of operational efficiency.

3.2. Thermoanalytical results

The TGA profile of the examined RDF samples generally exhibits four distinct stages: moisture vaporization, devolatilization, char combustion, and ash-related reactions. These stages are reflected in the DTG peaks as shown in Fig. 5, with the two major peaks corresponding to devolatilization and char combustion. The devolatilization around 300 °C is attributed to cellulose and hemicellulose materials, with a possible contribution from the early decomposition of specific plastics [44–46,48]. The char combustion peak in DTG presents a secondary shoulder, attributable to the oxidation of heterogeneous composition of RDF, including lignin and carbon backbones of plastics [48]. The offset of the char combustion peak is attributed to the burnout temperature. A smaller third DTG peak, markedly different between air and oxyfuel combustion, may be associated with ash-related processes such as calcination reactions. Similar observations have been made for MSW, where this stage was linked to inorganic salt decomposition, particularly calcium carbonate and shifted to higher temperature in CO_2/O_2 atmosphere [45,48]. In DTA profiles, three major exothermic but overlapping peaks are shown. The first two are assigned to the devolatilization and volatile combustion of different materials, while the third and highest peak corresponds to overall char combustion.

3.2.1. Impact of O_2 concentration

Overall, increasing the O_2 concentration in the OM causes the DTG curves to shift toward lower temperatures, indicating higher reactivity, as reflected in increased mass loss rates as shown in Fig. A.2. This trend is in line with numerous literature findings for MSW, coal, and biomass under oxyfuel conditions, e.g. [43,44,46,68].

The enhanced reactivity is particularly evident in the char combustion stage, whereas devolatilization is far less sensitive to O_2 enrichment. Increasing O_2 has slight effect on the maximum weight loss rate of devolatilization but significantly enhances the maximum weight loss rate of char combustion and advances its onset [Fig. A.2.]. A significant impact on ignition temperature of char combustion has been reported in literature [68–70].

As shown in Fig. 5 a) and b), the first DTG peak temperature remains essentially unchanged, while the char combustion peak and burnout temperature in DTG and DTA shift markedly with increasing O_2. These results align with previous studies on MSW, coal-biomass mixtures, and excavated waste, which consistently report minimal influence on devolatilization but strong effects on char combustion [43,48,71]. This was attributed to the fact that O_2 plays a limited role in the primary thermal breakdown of volatile-rich components, whereas chemical oxidation processes dominate in the char combustion. Chanca et al. reported that effects of increasing oxygen concentration are differently strong with coal and biomass, reflecting differences in their chemical structure [71]. This variability may explain the differing extents of the shift observed in the combustion peak temperature and the shoulder peak temperature, because RDF contains a range of materials with distinct oxidation behaviors. The strong shift of DTG and DTA combustion peak temperatures and burnout temperatures aligns with findings for other materials such as coal-biomass mixtures [68], MSW and low-rank semi-coke [44] and dried sewage sludge [70]. Quantitatively, matching air combustion conditions requires O_2 concentrations in CO_2 of 34.71 ± 2.15 vol.-% for the DTG shoulder of peak 2, 32.40 ± 2.03 vol.-% for the DTG burnout temperature, and 34.54 ± 2.11 vol.-% for the DTA char combustion peak, based on 95% confidence intervals (for correlations $R^2 > 0.8$). These values are slightly higher than the ~30 vol.-% O_2 threshold reported in several studies [10,69,70]. In conclusion, the present results confirm that O_2 enrichment primarily benefits char combustion, improving reactivity, lowering ignition and burnout temperatures, and shortening overall combustion time, while devolatilization is slightly accelerated.

3.2.2. Impact of H_2O concentration

The thermoanalytical measurements evaluate the impact of the varied H_2O concentration in the OM depending on the chosen FGR strategy. Overall, increasing the H_2O concentration in the OM causes a slight shift of DTG and DTA peaks toward lower temperatures (Fig. 5 c) and d)), indicating an increase in overall reactivity and, in some cases, higher mass loss rates (Fig. A.2). This behavior is consistent with literature findings for coal and biomass, where steam addition has been shown to enhance reactivity and shorten combustion time under O_2/CO_2 conditions [38]. The observed effect is modest compared to O_2 enrichment but still measurable, particularly during the char combustion stage. For devolatilization, the influence of H_2O is negligible. In the present experiments, neither the maximum weight loss rate nor the peak temperature of devolatilization changed significantly with increased water vapor content. These findings align with [35], who reported that steam addition in O_2/CO_2 atm had little to no effect on the devolatilization of biomass. In contrast, char combustion responds more noticeably to water vapor presence. In our experiments, higher H_2O concentrations led to a measurable increase in the maximum weight loss rate and a slight decrease in the onset temperature of char combustion as shown in Fig. A.2. This is consistent with small ignition time reductions reported in laboratory-scale studies on coal and biomass [27,31,32,34]. However, Escudero et al. [34] observed an ignition delay when steam concentration reached 40 vol.-%, indicating that the promoting effect of steam shows a maximum and may reverse beyond a certain threshold. The positive influence at moderate H_2O concentrations is likely due to the lower molar heat capacity and higher O_2 diffusivity of H_2O compared to CO_2, which enhance the oxidation process [27,35,36].

In line with previous studies [33,37,38], the overall reactivity of char increased more noticeably at lower O_2 levels, suggesting that steam can partially compensate for reduced oxygen availability. The DTG curves in this study show a slight shift of the char combustion peak and burnout temperature, while the DTA results indicate a more substantial reduction in burnout time. The relative mass loss at the burnout temperature, the burnout rate, showed no significant correlation with H_2O concentration (Fig. A.3). The heterogeneity of RDF, particularly variations in ash content, obscured potential effects attributable to water vapor. While char-H_2O reactions could prolong the burnout and reduce particle temperature, the produced gas phase products could promote combustion [30,31,40]. Literature reports on the impact of steam on burnout time and rate to be divergent, which remains subject for further investigation [27,30,32,33,36,39].

For the design of FGR in oxyfuel combustion, the high steam content in wet FGR appears to exert a slightly positive influence on char combustion under the tested conditions. Such an effect suggests that, in wet recirculation configurations, O_2 concentration and demand might be marginally reduced while maintaining similar combustion performance to dry conditions. However, the present findings also confirm that the effect of O_2 concentration on combustion parameters is substantially more pronounced than that of H_2O.

It should be noted that the modeling is based on a typical MSW composition with higher moisture content compared to the RDF used in

the experiments. However, the experimental evaluation focuses on characteristic combustion temperatures and does not consider the drying phase, i.e., the evaporation of moisture occurring at around 100 °C. Therefore, the results are expected to remain valid for transfer to waste compositions with higher moisture contents.

4. Conclusions and outlook

This study investigated the impact of different flue gas recirculation (FGR) strategies on combustion atmosphere and emissions, bridging the gap between experimental research and process modeling. An oxyfuel combustion model was developed and complemented with TGA/DTA experiments to assess gas composition, volume flow rate, and the sensitivity of key parameters, such as CO_2 and N_2 content in the flue gas to CO_2 compression and purification unit (CPU).

The investigated FGR strategies resulted in distinct volume flow rates and gas compositions. Wet recycling before the flue gas treatment (FGT) (Path A) provided high pollutant concentrations in the oxidizer mixture (OM), increasing risks of corrosion and plant outages, yet reduced the gas volume flow in FGT and flue gas condensation (FGC). Wet recirculation after FGT (Path B) significantly lowered pollutant levels in the OM, but, as Path A, exhibited very high H_2O concentrations in the OM, which is sensitive to the moisture content of MSW and the set O_2 concentration. Dry recirculation (Path C) yielded the highest CO_2 concentration in the flue gas to CPU, but also the highest N_2 content, mainly sourced from air leakage. The CO_2 content in flue gas to CPU is highly sensitive to the excess oxygen ratio. Path C required about 11.6% less O_2 than the wet FGR strategies because a larger absolute amount of O_2 is recirculated to the OM.

Thermoanalytical results confirmed a strong influence of O_2 concentration on combustion performance. Char combustion was significantly promoted by increased O_2 concentration, whereas devolatilization showed only minor sensitivity. Achieving similar char combustion and burnout temperatures as with air required O_2 concentrations in CO_2 of approximately 32–35 vol.-%. Further, increasing H_2O concentration up to 35 vol.-% slightly promoted char combustion, with negligible impact on devolatilization. Consequently, the high H_2O content in the OM of wet FGR may slightly enhance combustion, further supporting the applicability of this strategy. Future research will focus on advanced FGR concepts, alternative FGT technologies, and the energetic impacts of varying gas volume flows, alongside thermoanalytical investigations under different H_2O and O_2 concentrations.

CRediT authorship contribution statement

Isabel Kaphahn: Writing – review & editing, Writing – original draft, Visualization, Validation, Resources, Project administration, Methodology, Investigation, Funding acquisition, Formal analysis, Data curation, Conceptualization. **Peter Quicker:** Writing – review & editing, Validation, Supervision, Resources, Methodology, Funding acquisition, Conceptualization.

Declaration of generative AI and AI-assisted technologies in the writing process

During the preparation of this work the authors used ChatGPT in order to improve readability and linguistic clarity. After using this tool, the authors reviewed and edited the content as needed and take full responsibility for the content of the published article.

Funding

This work was supported by the Sustainable Industrial Society Foundation, Munich, Germany.

Declaration of competing interest

The authors declare that they have no known competing financial interests or personal relationships that could have appeared to influence the work reported in this paper.

Appendix A. Appendix

Detailed Model Description

In contrast to detailed process simulation approaches (e.g., Aspen Plus), which model the entire plant including auxiliary units and rely on extensive thermodynamic and kinetic sub-models, the present approach is based on a simplified mass balance framework. This allows for a transparent evaluation of different FGR strategies, while reducing the dependence on uncertain input parameters such as reaction kinetics or heat transfer correlations. The model is therefore not intended to replace detailed process simulations, but to provide a robust first-order assessment, to enable a consistent comparison of multiple FGR configurations, and to identify key influencing parameters as well as remaining research needs.

Oxyfuel combustion

Using a mass balance approach, the combustion calculation considers the elements C, H, S, Cl, N, O, inherent moisture, and non-combustible ash. Minor components typically found in MSW, such as fluor, heavy metals (e.g., Pb, Zn, Cd, Hg), and trace organic pollutants, are not considered. The waste composition is given by recognized guidelines VDI 3460 [62], representing a typical German MSW stream for WtE plants. The influence of fuel moisture is additionally addressed in the sensitivity analysis. The oxyfuel combustion is based on a stoichiometric combustion calculation (see eq. 2).

The fuel S to SO_2 degree of conversion is set as 100%, the amount of SO_3 is negligible [63]. This assumption represents an idealized upper bound, as full-scale measurements in waste incineration plants indicate that the majority of fuel sulfur (>75%)is released to the gas phase, predominantly as SO_2 [72].

The fuel Cl to HCl degree of conversion is assumed to be 100%. In practice, approximately 90% of fuel chlorine is released to the gas phase during grate combustion, mainly as HCl, with a smaller fraction remaining in bottom ash or forming alkali chlorides [72]. Both transfer coefficients are idealized but, for air combustion, have been proven to show realistic results regarding flue gas pollutant concentrations and are commonly applied in engineering combustion calculations being widely accepted for estimating flue gas compositions [63]. Due to the lack of reliable data on fuel-N to NO conversion under oxyfuel combustion conditions, a conversion rate of 15% is applied in this model. This value corresponds to experimentally observed conversion rates in conventional solid-fuel and waste combustion [73,74]. It should be noted that, in practice, these conversion rates may vary depending on fuel composition, combustion conditions, and reactor design. The selected assumptions are considered appropriate for a first-order assessment and for enabling a consistent comparison of different FGR strategies. A more detailed investigation of pollutant formation and conversion under oxyfuel conditions, particularly for waste-derived fuels, remains subject to future experimental studies.

The oxyfuel combustion calculation considers the FGR and its mixing with supplied oxygen and false air as shown in Fig. 1. Intermediate calculation formulas are listed in Table A.1. The model iterated on 100 FGR steps to achieve steady-state conditions. Convergence to a steady state was verified by ensuring that the gas composition remained constant up to the fifth decimal place between iterations 90 and 100. For the base scenario, the

variation in gas composition toward a steady state over the iteration steps is presented in Figure A.1. The model is regulated by the defined O_2 excess ratio and O_2-concentration in the OM. Both parameters are subsequently varied in the sensitivity analysis. The O_2 excess ratio is defined as the ratio of supplied oxygen to the stoichiometric oxygen requirement, as given by eq. 1. For the base scenario, it is defined as 1.8, which is a typical value for German WtE plants [75]. The oxygen concentration in the OM is defined as 30 vol.-%, reflecting the general consensus in the literature that this level of O_2 is required in oxyfuel combustion to achieve combustion characteristics similar to conventional air combustion [10]. As shown in Figure A.1., air is used in the first combustion calculation step, then, starting with the first FGR step, 30 vol-% O_2 is defined in the oxidizer mixture. Given the very high purity of O_2 produced by AEL electrolysis of 99–99.8% [76] and PEM electrolysis of 99,999% [77], the oxygen purity in this model is assumed to be 100%.

For a German WtE plant, false air entry across the overall process has been determined to reach up to 16 vol.-% of the combustion air, corresponding to approximately 11 vol.-% of the flue gas. [67]. In contrast, Kather et al. state that air leakage rates as low as 2–4 vol.-% of the flue gas for new power plants, increasing to around 10 vol.-% over time [78]. To account for this range, the false-air leakage in the present model is defined as 5 vol.-% of the OM and is subsequently used as a variation parameter in the sensitivity analysis. The false air composition is defined as 21 vol.-% O_2 and 79 vol.-% N_2. False air ingress is assumed to occur primarily at the front-end of the process, i.e., within the fuel feeding system. In particular, air entrained with the waste represents an inherent and largely unavoidable source of false air. In contrast, air leakages from downstream process units (e.g., membrane walls, compensators, sealing air, or auxiliary systems) can be significantly reduced through appropriate technical measures when implementing oxyfuel technology [79]. These contributions from downstream units are therefore not explicitly considered in the present model.

Different FGR configurations and therefore varying gas composition inherently influence the thermal conditions in the combustion chamber due to changes in heat capacity and gas dilution. In the present study, these temperature effects are not explicitly analyzed, as the focus is placed on the comparison of gas volume flows and gas compositions.

Flue gas treatment and condensation

The FGT consists of a dry sorption process using $NaHCO_3$ and activated carbon. The reaction equations of $NaHCO_3$ with HCl and SO_2 and their respective degrees of conversion of 92.30% and 99.30% are taken from the literature [63], as well as the molar fractions of the resulting $NaSO_3$ (70 mol-%) and $NaSO_4$ (30 mol-%). The stoichiometric amount of added $NaHCO_3$ is 1.2, which is assumed to completely activate to form Na_2CO_3 [63]. The solid reaction products and the ash are removed from the process via the bag filter. The NO_x reduction is accounted for by a tail-end SCR system, which is commonly applied in WtE plants, as the gas stream is low in particulate matter when entering the catalyst. The introduced NH_4OH solution contains 25 w.-% NH_3 in H_2O. The NH_3 stoichiometric ratio is assumed to be 1 to achieve 75% NO-reduction. The NH_3 slip in industrial SCR operation is very low (e.g. 4 $mg/m^3_{N,\ dry}$ [63]), and is therefore not considered in this model.

In the FGC, a fixed 85% H_2O removal efficiency is used as a simplified but realistic representation of condenser performance, consistent with values reported in other simulations (e.g. [57,59]). Consequently, the amount of condensed H_2O varies with the upstream moisture content as seen in Fig. 3, which is a reasonable first-order approximation for evaluating gas-composition trends rather than replicating real condenser design. It is acknowledged that condensation depends on temperature and saturation vapor pressure. In practice, flue gas condensation systems are designed based on temperature levels and overall energy integration, which are not explicitly considered here and will be subject to future work.

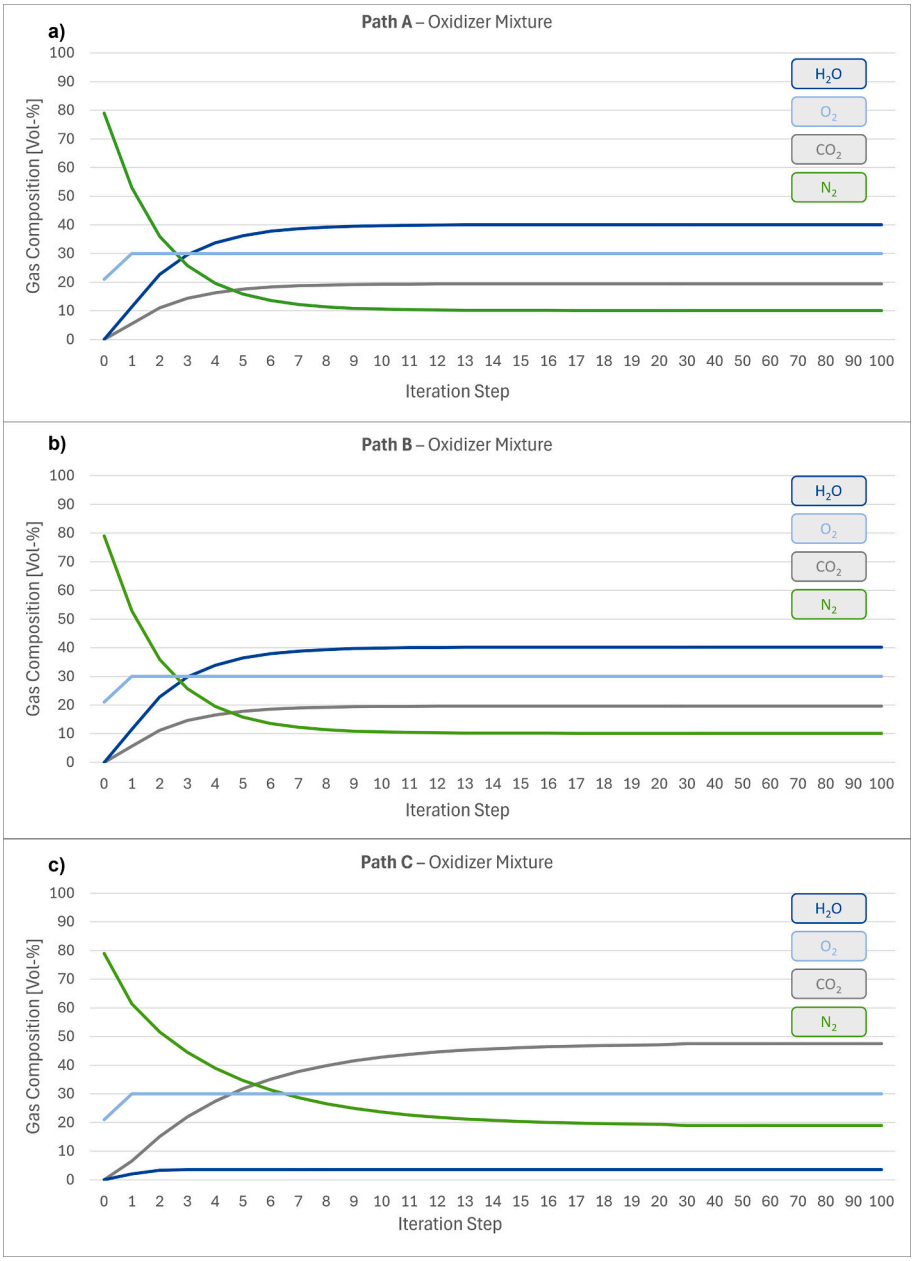


Fig. A.1. Gas composition of OM as a function of iteration step for FGR a) Path A, b) Path B and c) Path C.

Table A.1
Intermediate values calculated in the stoichiometric oxyfuel combustion model.

Parameter	Unit	Formula	Equation
		Ideal Combustion Calculation	
Empirical Elemental Coefficients (p, q, r, s, t, u)	$kmol/kg_{waste}$	$\text{e.g. } p = \frac{x_c}{M_c}$	(3)
Stoichiometric Oxygen Demand	$kmol_{O2}/kg_{waste}$	$v_{O_2O} = p + \frac{q-u}{4} + r + \frac{s*15\%}{2} - \frac{t}{2}$	(4)
Actual Oxygen Demand	$kmol_{O2}/kg_{waste}$	$v_{O_2} = v_{O_2O} \bullet \lambda$	(5)
Actual Oxidizer Mixture Demand	$kmol_{gas}/kg_{waste}$	$v_{OM} = \frac{v_{O_2}}{y_{O_2,OM}}$	(6)
Actual Oxidizer Mixture Demand	kg_{gas}/kg_{waste}	$\mu_{OM} = \frac{v_{OM}}{M_{OM}}$	(7)
Specific Mass of Flue Gas [State A]	kg_{gas}/kg_{waste}	$\mu_{G,A} = \mu_{OM} + 1 - a$	(8)
Fraction of CO_2 in Flue Gas [State A]	[wt.-%]	$x_{CO_2,A} = \frac{p*M_{CO_2} + \mu_{OM}*x_{CO_2,OM}}{\mu_{G,A}}$	(9)

(*continued on next page*)

Table A.1 (*continued*)

Parameter	Unit	Formula	Equation
Fraction of H_2O in Flue Gas [State A]	[wt.-%]	$x_{H_2O,A} = \frac{\frac{q-u}{2}*M_{H_2O} + w + \mu_{OM}*x_{H_2O,OM}}{\mu_{G,A}}$	(10)
Fraction of HCl in Flue Gas [State A]	[wt.-%]	$x_{HCl,A} = \frac{u*M_{HCl} + \mu_{OM}*x_{HCl,OM}}{\mu_{G,A}}$	(11)
Fraction of NO in Flue Gas [State A]	[wt.-%]	$x_{NO,A} = \frac{s*15\%*M_{NO} + \mu_{OM}*y_{NO,OM}}{\mu_{G,A}}$	(12)
Fraction of SO_2 in Flue Gas [State A]	[wt.-%]	$x_{SO_2,A} = \frac{p*M_{SO_2} + \mu_{OM}*x_{SO_2,OM}}{\mu_{G,A}}$	(13)
Fraction of N_2 in Flue Gas [State A]	[wt.-%]	$x_{N_2,A} = \frac{s/2*85\%*M_{N_2} + \mu_{OM}*x_{N_2,OM}}{\mu_{G,A}}$	(14)
Fraction of O_2 in Flue Gas [State A]	[wt.-%]	$x_{O_2,A} = \frac{v_{O_2O}*(\lambda-1)}{\mu_{G,A}}$	(15)
Amount of Gas in Flue Gas [State A]	$kmol_{gas}/kg_{waste}$	e.g. $n_{O_2,A} = y_{O_2,A}*v_{G,A}$	(15)
	Flue Gas Treatment		(16)
Stoichiometric Amount of $NaHCO_3$	$kmol_{NaHCO3}/kg_{waste}$	$n_{NaHCO_3} = \left(n_{HCl,A}*99.33\% + n_{SO_2,A}*99.33\%*2\right)$	(17)
Stoichiometric Amount of NH_3	$kmol_{NH3}/kg_{waste}$	$n_{NH_3} = 75\%*n_{NO}$	(18)
Amount of CO_2 in Clean Flue Gas [State B]	$kmol_{CO2}/kg_{waste}$	$n_{CO_2,B} = n_{CO_2,A} + 0.5n_{NaHCO_3}*1.2 + \frac{n_{HCl}*99.33\%}{2} + n_{SO2}*92.30\%$	(19)
Amount of H_2O in Clean Flue Gas [State B]	$kmol_{H2O}/kg_{waste}$	$n_{H_2O,B} = n_{H_2O,A} + 0.5n_{NaHCO_3}*1.2 + 0.5*99.33\%n_{HCl} + n_{NH_3}*1.5 + 2.84\, n_{NH_3}$	(20)
Amount of HCl in Clean Flue Gas [State B]	$kmol_{HCl}/kg_{waste}$	$n_{HCL,B} = n_{HCL,A}*(1-99.33\%)$	(21)
Amount of NO in Clean Flue Gas [State B]	$kmol_{NO}/kg_{waste}$	$n_{NO,B} = n_{NO,A}*(1-75\%)$	(22)
Amount of SO_2 in Clean Flue Gas [State B]	$kmol_{NO}/kg_{waste}$	$n_{SO_2,B} = n_{SO_2,A}*(1-92.30\%)$	(23)
Amount of N_2 in Clean Flue Gas [State B]	$kmol_{N2}/kg_{waste}$	$n_{N_2,B} = n_{N_2,A} + n_{NH_3}$	(24)
Amount of O_2 in Clean Flue Gas [State B]	$kmol_{N2}/kg_{waste}$	$n_{O_2,B} = n_{O_2,A} - \frac{0,3*n_{SO_2,A}*92.30\%}{2} - \frac{n_{NH_3}}{4}$	(25)
Specific Amount of Clean Flue Gas [State B]	$kmol_{gas}/kg_{waste}$	$v_{G,B} = n_{CO_2,B} + n_{H_2O,B} + n_{HCL,B} + n_{NO,B} + n_{SO_2,B} + n_{N_2,B} + n_{O_2,B}$	(26)
Share of Gas in Clean Flue Gas	[vol.-%]	$y_{O_2,B} = \frac{n_{O_2,B}}{v_{G,B}}$	(26)
	Flue Gas Condensation		
Amount of H_2O in Clean, Dry Flue Gas [State C]	$kmol_{H2O}/kg_{waste}$	$n_{H_2O,C} = n_{H_2O,B}*(1-85\%)$	(28)
Amount of non-H_2O Gases in Clean, Dry Flue Gas [State C]	$kmol_{gas}/kg_{waste}$	$e.g. n_{O_2,C} = n_{O_2,B}$	(29)
Specific Amount of Clean, Dry Flue Gas [State C]	$kmol_{gas}/kg_{waste}$	$v_{G,C} = n_{CO_2,C} + n_{H_2O,C} + n_{HCL,C} + n_{NO,C} + n_{SO_2,C} + n_{N_2,C} + n_{O_2,C}$	(30)
Share of Gas in Clean, Dry Flue Gas	[vol.-%]	$y_{O_2,C} = \frac{n_{O_2,C}}{v_{G,C}}$	(31)
	Flue Gas Recirculation		
Oxygen Fraction in OM	[vol.-%]	$y_{O_2,OM} = 30\ vol\% = y_{O_2,Recirculated,OM} + y_{O_2,AirLeakage,OM} + y_{O_2,Supply,OM}$	(32)
Non-O_2 Fraction in OM	[vol.-%]	$y_{Non-O_2,OM} = 70\ vol\% = y_{Non-O_2,Recirculated,OM} + y_{N_2,AirLeakage,OM}$	(33)
Recirculation Rate [with i = FGR Strategy = A, B, C]	[vol.-%]	$R_i = \frac{y_{Non-O_2,Recirculated,OM}*v_{G,OM}}{v_{G,i}}$	(34)
Amount of Flue Gas in Process after Recirculation	$kmol_{Gas}/kg_{waste}$	$v_{G,i'} = v_{G,i}*(1-R_i)$	(35)

Appendix B. Supplementary Thermoanalytical Results

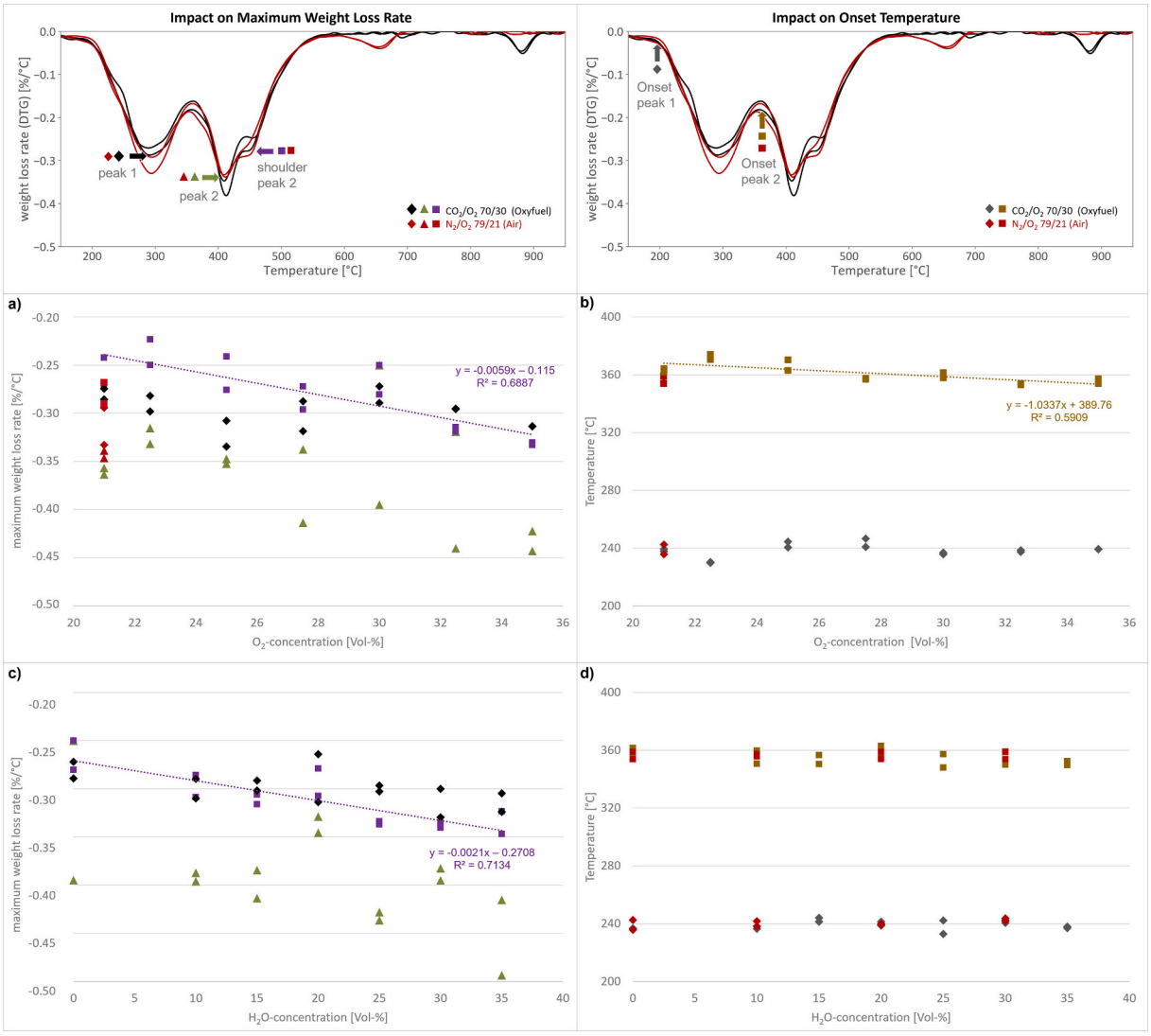


Fig. A.2. DTG Analysis of a) impact of O_2-concentraion on maximum weight loss rate, b) impact of O_2-concentraion on onset temperature, c) impact of H_2O-concentraion on maximum weight loss rate at constant O_2-concentration, d) impact of H_2O on onset temperature at constant O_2-concentration.

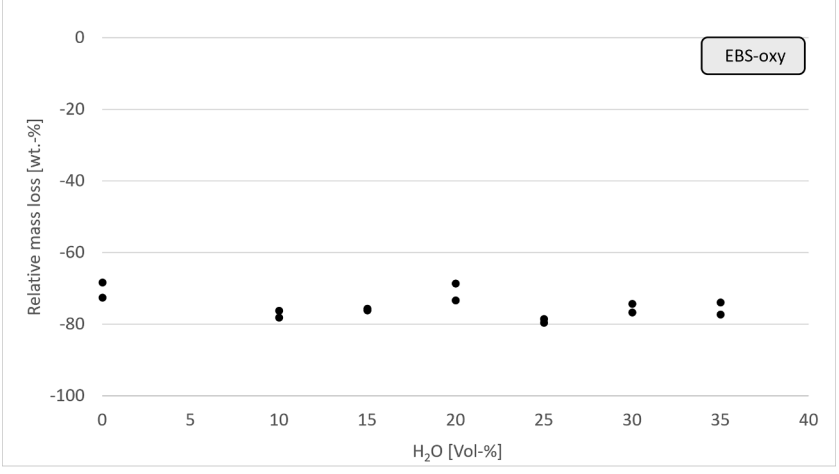


Fig. A.3. DTG Analysis of impact of H_2O concentration on mass loss rate at burnout temperature.

Data availability

The data presented in this study are available on request from the corresponding author due to privacy concerns.

References

[1] European Parliament, Reducing carbon emissions: EU targets and policies, Available from: https://www.europarl.europa.eu/topics/de/article/20180305STO99003/reduktion-von-co2-emissionen-ziele-und-massnahmen-der-eu, 2026.

[2] ASA, Statusbericht der deutschen Kreislaufwirtschaft 2024 [Status Report on the German Circular Economy 2024] [in German], Available from, https://statusbericht-kreislaufwirtschaft.de/wp-content/uploads/2024/01/Statusbericht_2024_25012024_opt.pdf, 2026.

[3] F. Poretti, E. Stengler, The Climate Roadmap of the European Waste-to-Energy Sector The path to Carbon Negative, in: IEA Greenhouse Gas R&D Programme, Greenhouse Gas Control Technologies, 2022, p. 16.

[4] Eurostat, Municipal waste statistics, Available from, https://ec.europa.eu/eurostat/statistics-explained/index.php?title=Municipal_waste_statistics#Municipal_waste_generation, 2025.

[5] CEWEP, Waste-to-Energy Plants in Europe in 2022, Available from, https://www.cewep.eu/waste-to-energy-plants-in-europe-in-2022/, 2026.

[6] W. Dietz, M. Schönemann, M. Seitz, N. Thiel, W. Rommel, Nutzungsmöglichkeiten und Potenziale bei Abfallbehandlungsanlagen zur Sektorenkopplung, Energiebereitstellung und CO_2-Abscheidung [Possible applications and potentials for sector coupling, energy supply and CO_2 capture in waste treatment plants] [in German] [July 09, 2026]; Available from: https://www.uba.de/n111369de, 2024.

[7] K. Arnold, A. Scholz, A. Taubitz, H. Wilts, Unvermeidbare Emissionen aus der Abfallbehandlung – Optionen auf dem Weg zur Klimaneutralität [Unavoidable emissions from waste treatment – options on the path to climate neutrality] [in German]. In: Energiewirtschaftliche Tagesfragen, Available from: https://epub.wupperinst.org/frontdoor/deliver/index/docId/8028/file/8028_Arnold.pdf, 2026.

[8] D. Münter, H. Fehrenbach, T. Fröhlich, Optionen und Potenziale für die Nutzung von biogenem CO_2 für die Herstellung von strombasierten erneuerbaren Energieträgern [Options and Potential for the Use of Biogenic CO2 as a Feedstock for the Production of Electricity-based Renewable Fuels] [in German]. Umweltbundesamt, 2025, https://doi.org/10.60810/openumwelt-7849.

[9] L. Acampora, S. Grilletta, G. Costa, The Integration of Carbon Capture, Utilization, and Storage (CCUS) in Waste-to-Energy Plants: A Review, Energies 18 (8) (2025) 1883, https://doi.org/10.3390/en18081883.

[10] P. Wienchol, A. Szlęk, M. Ditaranto, Waste-to-energy technology integrated with carbon capture – Challenges and opportunities, Energy (2020) 198, https://doi.org/10.1016/j.energy.2020.117352.

[11] D. Kearns, Waste-to-Energy with CCS: A pathway to carbon-negative power generation, Available from: https://www.globalccsinstitute.com/wp-content/uploads/2025/08/Waste-to-Energy-Perspective_October-2019-5.pdf, 2026.

[12] S. Yadav, S.S. Mondal, A review on the progress and prospects of oxy-fuel carbon capture and sequestration (CCS) technology, Fuel (2022) 308, https://doi.org/10.1016/j.fuel.2021.122057.

[13] M.B. Toftegaard, J. Brix, P.A. Jensen, P. Glarborg, A.D. Jensen, Oxy-fuel combustion of solid fuels, Prog. Energy Combust. Sci. 36 (5) (2010) 581–625, https://doi.org/10.1016/j.pecs.2010.02.001.

[14] M. Bailera, P. Lisbona, B. Peña, L.M. Romeo, Energy Storage, Springer International Publishing, Cham, 2020.

[15] J. Brellochs, OxyCO2 - Oxyfuel combustion of sewage sludge with electrolysis O2 for the utilization of CO2 in Power-to-X processes, Available from: https://www.zsw-bw.de/en/projects/circular-economy/oxyco2-oxyfuel-combustion-of-sewage-sludge-with-electrolysis-o2-for-the-utilization-of-co2-in-power-to-x-processes.html, 2025.

[16] J. Jeddizahed, P.A. Webley, T.J. Hughes, Integrating alkaline electrolysis with oxyfuel combustion for hydrogen and electricity production, Appl. Energy 361 (2024) 122856, https://doi.org/10.1016/j.apenergy.2024.122856.

[17] S. Yun, J. Lee, H. Cho, J. Kim, Oxy-fuel combustion-based blue hydrogen production with the integration of water electrolysis, Energy Convers. Manag. 291 (2023) 117275, https://doi.org/10.1016/j.enconman.2023.117275.

[18] Y. Huang, Y. Jiang, Z. Tong, Design optimization of oxygen-fuel combustion system of municipal solid waste driven by electrolytic oxygen production from renewable energy, J. Clean. Prod. (2024) 142883, https://doi.org/10.1016/j.jclepro.2024.142883.

[19] M. Re, S. Li, T. Laukkanen, M. Järvinen, Profitability analysis of H2 production by water electrolysis in an integrated oxy-fuel combustion thermal power plant, Fuel 398 (2025) 135544, https://doi.org/10.1016/j.fuel.2025.135544.

[20] S. Peng, Y. Tang, J. Tang, X. Wang, X. Liang, H. Huang, et al., Renewable dimethyl ether production un-der the integration from municipal solid waste oxy-fuel combustion and water electrolyze: In-sights from advanced exergy and exergoeconomic perspectives, Int. J. Hydrog. Energy 141 (2025) 253–265, https://doi.org/10.1016/j.ijhydene.2025.05.385.

[21] R. Stanger, T. Wall, R. Spörl, M. Paneru, S. Grathwohl, M. Weidmann, et al., Oxyfuel combustion for CO2 capture in power plants, Int. J. Greenh. Gas Con. 40 (2015) 55–125, https://doi.org/10.1016/j.ijggc.2015.06.010.

[22] D. Adams, Flue Gas Treatment for CO2 capture, Available from: https://usea.org/sites/default/files/062010_Flue%20gas%20treatment%20for%20co2%20capture_ccc169.pdf, 2025.

[23] G. Pipitone, O. Bolland, Power generation with CO2 capture: Technology for CO2 purification, Int. J. Greenh. Gas Con. 3 (5) (2009) 528–534, https://doi.org/10.1016/j.ijggc.2009.03.001.

[24] V. White, L. Torrente-Murciano, D. Sturgeon, D. Chadwick, Purification of oxyfuel-derived CO2, Energy Procedia 1 (1) (2009) 399–406, https://doi.org/10.1016/j.egypro.2009.01.054.

[25] A. Darde, R. Prabhakar, J.-P. Tranier, N. Perrin, Air separation and flue gas compression and purification units for oxy-coal combustion systems, Energy Procedia 1 (1) (2009) 527–534, https://doi.org/10.1016/j.egypro.2009.01.070.

[26] B. Buhre, L.K. Elliott, C.D. Sheng, R.P. Gupta, T.F. Wall, Oxy-fuel combustion technology for coal-fired power generation, Prog. Energy Combust. Sci. 31 (4) (2005) 283–307, https://doi.org/10.1016/j.pecs.2005.07.001.

[27] K. Lei, R. Zhang, B. Ye, J. Cao, D. Liu, Combustion of single particles from sewage sludge/pine sawdust and sewage sludge/bituminous coal under oxy-fuel conditions with steam addition, Waste Manag. 101 (2020) 1–8, https://doi.org/10.1016/j.wasman.2019.09.034.

[28] S. Chen, Fundamentals of Oxy-fuel Combustion, in: Oxy-Fuel Combustion, Elsevier, 2018, pp. 13–30.

[29] H. Liu, Y. Shao, Predictions of the impurities in the CO2 stream of an oxy-coal combustion plant, Appl. Energy 87 (10) (2010) 3162–3170, https://doi.org/10.1016/j.apenergy.2010.04.014.

[30] C. Bu, A. Gómez-Barea, B. Leckner, X. Wang, J. Zhang, G. Piao, The effect of H2O on the oxy-fuel combustion of a bituminous coal char particle in a fluidized bed: Experiment and modeling, Combust. Flame. 218 (2020) 42–56, https://doi.org/10.1016/j.combustflame.2020.03.025.

[31] R.B. Kops, F.M. Pereira, M. Rabaçal, M. Costa, Effect of steam on the single particle ignition of solid fuels in a drop tube furnace under air and simulated oxy-fuel conditions, Proc. Combust. Inst. 37 (3) (2019) 2977–2985, https://doi.org/10.1016/j.proci.2018.05.091.

[32] J. Riaza, L. Álvarez, M.V. Gil, C. Pevida, J.J. Pis, F. Rubiera, Effect of oxy-fuel combustion with steam addition on coal ignition and burnout in an entrained flow reactor, Energy 36 (8) (2011) 5314–5319, https://doi.org/10.1016/j.energy.2011.06.039.

[33] B. Yi, L. Zhang, F. Huang, Z. Mao, C. Zheng, Effect of H 2 O on the combustion characteristics of pulverized coal in O 2 /CO 2 atmosphere, Appl. Energy 132 (2014) 349–357, https://doi.org/10.1016/j.apenergy.2014.07.031.

[34] A.I. Escudero, M. Aznar, L.I. Díez, M.C. Mayoral, J.M. Andrés, From O2/CO2 to O2/H2O combustion: The effect of large steam addition on anthracite ignition, burnout and NOx formation, Fuel Process. Technol. 206 (2020) 106432, https://doi.org/10.1016/j.fuproc.2020.106432.

[35] E. Marek, B. Świątkowski, Experimental studies of single particle combustion in air and different oxy-fuel atmospheres, Appl. Therm. Eng. 66 (1–2) (2014) 35–42, https://doi.org/10.1016/j.applthermaleng.2014.01.070.

[36] L.I. Díez, A. García-Mariaca, E. Llera-Sastresa, P. Canalís, On the oxy-combustion of blends of coal and agro-waste biomass under dry and wet conditions, Fuel 365 (2024) 131265, https://doi.org/10.1016/j.fuel.2024.131265.

[37] C. Dueso, M.C. Mayoral, B. Rubio, J.M. Andres, Oxy-steam combustion of torrefied biomass under high water vapor concentrations, in: GHGT-16. Lyon, France, 2022.

[38] M.V. Gil, J. Riaza, L. Álvarez, C. Pevida, J.J. Pis, F. Rubiera, A study of oxy-coal combustion with steam addition and biomass blending by thermogravimetric analysis, J. Therm. Anal. Calorim. 109 (1) (2012) 49–55, https://doi.org/10.1007/s10973-011-1342-y.

[39] L.I. Díez, A. García-Mariaca, P. Canalís, E. Llera, Oxy-combustion characteristics of torrefied biomass and blends under O2/N2, O2/CO2 and O2/CO2/H2O atmospheres, Energy 284 (2023) 128559, https://doi.org/10.1016/j.energy.2023.128559.

[40] E.S. Hecht, C.R. Shaddix, M. Geier, A. Molina, B.S. Haynes, Effect of CO2 and steam gasification reactions on the oxy-combustion of pulverized coal char, Combust. Flame. 159 (11) (2012) 3437–3447, https://doi.org/10.1016/j.combustflame.2012.06.009.

[41] M. Becidan, M. Ditaranto, P. Carlsson, J. Bakken, M.N.P. Olsen, J. Stuen, Oxyfuel Combustion of a Model MSW—An Experimental Study, Energies 14 (17) (2021), https://doi.org/10.3390/en14175297.

[42] M. Jurczyk, M. Mikus, Krzysztof Dziedzic, flue gas cleaning in municipal waste-to-energy plants - Part I, Infrastruct. Ecol. Terr. IV (1) (2016), https://doi.org/10.14597/infraeco.2016.4.1.086.

[43] Z. Lai, X. Ma, Y. Tang, H. Lin, A study on municipal solid waste (MSW) combustion in N2/O2 and CO2/O2 atmosphere from the perspective of TGA, Energy 36 (2) (2011) 819–824, https://doi.org/10.1016/j.energy.2010.12.033.

[44] G. Ding, B. He, H. Yao, Y. Cao, L. Su, Z. Duan, Co-combustion behaviors of municipal solid waste and low-rank coal semi-coke in air or oxygen/carbon dioxide atmospheres, J. Therm. Anal. Calorim. 143 (1) (2021) 619–635, https://doi.org/10.1007/s10973-019-09170-z.

[45] Y. Tang, X. Ma, Z. Lai, Thermogravimetric analysis of the combustion of microalgae and microalgae blended with waste in N2/O2 and CO2/O2 atmospheres, Bioresour. Technol. 102 (2) (2011) 1879–1885, https://doi.org/10.1016/j.biortech.2010.07.088.

[46] Y. Tang, X. Ma, Z. Lai, Y. Fan, Thermogravimetric analyses of co-combustion of plastic, rubber, leather in N2/O2 and CO2/O2 atmospheres, Energy 90 (2015) 1066–1074, https://doi.org/10.1016/j.energy.2015.08.015.

[47] Y. Tang, X. Ma, Z. Lai, D. Zhou, Y. Chen, Thermogravimetric characteristics and combustion emissions of rubbers and polyvinyl chloride in N2/O2 and CO2/O2 atmospheres, Fuel 104 (2013) 508–514, https://doi.org/10.1016/j.fuel.2012.06.047.

[48] J. Lv, B. Yan, S. Zhou, Z. Wu, X. Liu, S. Lu, et al., Ignition, combustion and pollutant emissions characteristics of excavated waste in low oxygen concentration and O2/

CO2 atmosphere, Waste Manag. 200 (114770) (2025), https://doi.org/10.1016/j.wasman.2025.114770.
[49] Y. Tang, X. Ma, Z. Lai, D. Zhou, H. Lin, Y. Chen, NOx and SO2 emissions from municipal solid waste (MSW) combustion in CO2/O2 atmosphere, Energy 40 (1) (2012) 300–306, https://doi.org/10.1016/j.energy.2012.01.070.
[50] Y. Tang, X. Ma, C. Zhang, Q. Yu, Y. Fan, Effects of sorbents on the heavy metals control during tire rubber and polyethylene combustion in CO 2 /O 2 and N 2 /O 2 atmospheres, Fuel 165 (2016) 272–278, https://doi.org/10.1016/j.fuel.2015.10.038.
[51] Y. Tang, X. Ma, Q. Yu, C. Zhang, Z. Lai, X. Zhang, Heavy metal enrichment characteristics in ash of municipal solid waste combustion in CO2/O2 atmosphere, Waste Manag. 43 (2015) 247–254, https://doi.org/10.1016/j.wasman.2015.06.024.
[52] C. Ke, X. Ma, Y. Tang, W. Zheng, Z. Wu, The volatilization of heavy metals during *co*-combustion of food waste and polyvinyl chloride in air and carbon dioxide/oxygen atmosphere, Bioresour. Technol. 244 (Pt 1) (2017) 1024–1030, https://doi.org/10.1016/j.biortech.2017.08.075.
[53] C. Ke, X. Ma, Y. Tang, F. Tang, W. Zheng, Effects of natural and modified calcium-based sorbents on heavy metals of food waste under oxy-fuel combustion, Bioresour. Technol. 271 (2019) 251–257, https://doi.org/10.1016/j.biortech.2018.09.109.
[54] M. Dai, Z. Yu, Y. Tang, X. Ma, HCl emission and capture characteristics during PVC and food waste combustion in CO2/O2 atmosphere, J. Energy Inst. 93 (3) (2020) 1036–1044, https://doi.org/10.1016/j.joei.2019.09.004.
[55] J. Moreno, M. Schmid, S. Scharr, G. Scheffknecht, Oxy-Combustion of Solid Recovered Fuel in a Semi-Industrial CFB Reactor: On the Implications of Gas Atmosphere and Combustion Temperature, ACS Omega 7 (10) (2022) 8950–8959, https://doi.org/10.1021/acsomega.1c07334.
[56] A. Mack, J. Maier, G. Scheffknecht, Experimental investigation of oxyfuel combustion of RDF and wood chips in a grate incineration system, Int. J. Energy Clean Environ. 24 (8) (2023) 89–106, https://doi.org/10.1615/InterJEnerCleanEnv.2023046576.
[57] C. Fu, M. Ditaranto, M. Becidan, D. Berstad, J. Stuen, Conceptual design and process assessment of a MSW waste-to-energy plant with oxy-combustion CO 2 capture, Carbon Manag. 16 (1) (2025), https://doi.org/10.1080/17583004.2025.2473913.
[58] P. Copik, A. Szlęk, M. Ditaranto, Simplified mathematical model of oxy-fuel combustion of municipal solid waste in the grate furnace: effect of different flue gas recirculation rates and comparison with conventional mode, Arch. Thermodyn. (2024) 13–25, https://doi.org/10.24425/ather.2024.151233.
[59] G. Ding, B. He, Y. Cao, C. Wang, L. Su, Z. Duan, et al., Process simulation and optimization of municipal solid waste fired power plant with oxygen/carbon dioxide combustion for near zero carbon dioxide emission, Energy Convers. Manag. 157 (2018) 157–168, https://doi.org/10.1016/j.enconman.2017.11.087.
[60] G. Vilardi, N. Verdone, Exergy analysis of municipal solid waste incineration processes: The use of O2-enriched air and the oxy-combustion process, Energy 239 (2022) 122147, https://doi.org/10.1016/j.energy.2021.122147.
[61] Y. Sun, Waste oxy-fuel combustion integrated with supercritical CO2 cycle and high-temperature electrolysis technologies for e-methanol production: A feasibility analysis, Process Saf. Environ. Prot. 185 (2024) 225–238, https://doi.org/10.1016/j.psep.2024.02.086.
[62] Verein Deutscher Ingenieure. Emissionsminderung Thermische Abfallbehandlung: Grundlagen [Emission control Thermal waste treatment Fundamentals] [in German] (VDI 3460, Blatt1:2014–02), Düsseldorf, 2026.
[63] M. Beckmann, R. Karpf, V. Dütge, T. Wen, Vergleichende ökonomische Betrachtung verschiedener Einsatzstoffe bei Trockensorptionsverfahren zur Abgasreinigung [A comparative economic analysis of various feedstocks used in dry sorption processes for flue gas treatment] [in German], in: K.J. Thomé-Kozmiensky, M. Beckmann (Eds.), Energie aus Abfall, TK Verl. Karl Thomé-Kozmiensky, Neuruppin, 2011, pp. 583–631.
[64] United Nations Environment Programme, International Resource Panel. Global Resources Out-look 2024: Bend the Trend: Pathways to a liveable planet as resource use spikes. Nairobi, 2024.
[65] A.C. Caputo, M.P. Pelagagge, P. Salini, Heat exchanger design based on economic optimization, Available from: https://abcm.org.br/anais/encit/2006/arquivos/Thermal%20Systems/CIT06-0387.pdf, 2026.
[66] M. Ditaranto, CAPEWASTE project: Enabling carbon capture with oxy-fuel combustion technology for the Waste-to-Energy sector, in: IEA Greenhouse Gas R&D Programme, Greenhouse Gas Control Technologies, 2022, p. 16.
[67] M. Zwiellehner, VOKos – Effizienzsteigerung durch verfahrenstechnisch optimierende Korrosions-schutzkonzepte in Verbrennungsanlagen mit heterogenen Festbrennstoffen: Abschlussbericht [VOkos - Improving efficiency through process-optimising corrosion protection concepts in combustion plants using heterogeneous solid fuels: final report] [in German], Available from: https://www.gks-sw.de/images/forschungsberichte/VOKos-Schlussbericht-2017_10_31-SAR.pdf, 2025.
[68] S. Ahn, G. Choi, D. Kim, The effect of wood biomass blending with pulverized coal on combustion characteristics under oxy-fuel condition, Biomass Bioenergy 71 (2014) 144–154, https://doi.org/10.1016/j.biombioe.2014.10.014.
[69] Z. Lai, X. Ma, Y. Tang, H. Lin, Y. Chen, Thermogravimetric analyses of combustion of lignocellulosic materials in N2/O2 and CO2/O2 atmospheres, Bioresour. Technol. 107 (2012) 444–450, https://doi.org/10.1016/j.biortech.2011.12.039.
[70] S. Niu, M. Chen, Y. Li, F. Xue, Evaluation on the oxy-fuel combustion behavior of dried sewage sludge, Fuel 178 (2016) 129–138, https://doi.org/10.1016/j.fuel.2016.03.053.
[71] O. Chansa, Z. Luo, C. Yu, Study of the kinetic behavior of biomass and coal during oxyfuel co-combustion, Chin. J. Chem. Eng. 28 (7) (2020) 1796–1804, https://doi.org/10.1016/j.cjche.2020.02.023.
[72] M. Bøjer, P.A. Jensen, F. Frandsen, K. Dam-Johansen, O.H. Madsen, K. Lundtorp, Alkali/Chloride re-lease during refuse incineration on a grate: Full-scale experimental findings, Fuel Process. Technol. 89 (5) (2008) 528–539, https://doi.org/10.1016/j.fuproc.2007.10.003.
[73] P. Abelha, Combustion of poultry litter in a fluidised bed combustor, Fuel 82 (6) (2003) 687–692, https://doi.org/10.1016/S0016-2361(02)00317-4.
[74] Y.A. Levendis, A. Atal, J.B. Carlson, M.D. Quintana, PAH and soot emissions from burning components of medical waste: examination/surgical gloves and cotton pads, Chemosphere 42 (5–7) (2001) 775–783, https://doi.org/10.1016/s0045-6535(00)00251-4.
[75] M. Beckmann, Beschreibung unterschiedlicher Techniken und deren Entwicklungspotentiale zur Minderung von Stickstoffoxiden im Abgas von Abfallverbrennungsanlagen und Ersatzbrennstoff-Kraftwerken hinsichtlich Leistungsfähigkeit, Kosten und Energieverbrauch [Description of various techniques and their potential for reducing nitrogen oxides in the flue gas from waste incineration plants and substitute fuel power stations, in terms of performance, costs and energy consumption] [in German], Dessau-Roßlau, 2011. https://www.uba.de/n8160de.
[76] M. Holst, S. Aschbrenner, T. Smolinka, C. Voglstätter, G. Grimm, Cost forecast for low temperature electrolysis: Technology driven bottom-up prognosis for PEM and alkaline water electrolysis systems, Available from: https://www.ise.fraunhofer.de/content/dam/ise/de/documents/publications/studies/cost-forecast-for-low-temperature-electrolysis.pdf, 2026.
[77] S. Shiva Kumar, H. Lim, An overview of water electrolysis technologies for green hydrogen production, Energy Rep. 8 (2022) 13793–13813, https://doi.org/10.1016/j.egyr.2022.10.127.
[78] A. Kather, G. Scheffknecht, The oxycoal process with cryogenic oxygen supply, Naturwissenschaften 96 (9) (2009) 993–1010, https://doi.org/10.1007/s00114-009-0557-2.
[79] H. Anger, S. Staub, R. Koralewska, M. Schönsteiner, F. Sphöhrer, R. Prade, et al., CO2-Einsatz in der thermischen Abfallverwertung [The use of CO_2 in thermal waste treatment] [in German], in: S. Thiel, E. Thomé-Kozmiensky, P. Quicker, A. Gosten (Eds.), Abfallwirtschaft und Energie Band 1, TK-Verlag, Neuruppin, 2024.

Glossary

AEL: Alkaline Electrolysis
ASU: Air Separation Unit
CEWEP: Confederation of European Waste-to-Energy Plants
CFB: Circulating Fluidized Bed
CIUDEN: Fundaciòn Ciudad de la Energia
CPU: Compression and Purification Unit
DTA: Differential Thermal Analysis
DTG: Derivative Thermogravimetry
FGR: Flue Gas Recirculation
FGT: Flue Gas Treatment
MEA: Monoethanolamine
MSW: Municipal Solid Waste
OM: Oxidizer Mixture
PC: Pulverized Coal
PEM: Proton Exchange Membrane
RDF: Refuse Derived Fuel
SCR: Selective Catalytic Reduction
SNCR: Selective Non-Catalytic Reduction
SRF: Solid Recovered fuel
TGA: Thermogravimetric Analysis
WtE: Waste to Energy